JCIM JOURNAL OF CHEMICAL INFORMATION AND MODELING

Article

Cite This: J. Chem. Inf. Model. 2020, 60, 747−755

pubs.acs.org/jcim

On the Interpretation of subtilisin Carlsberg Time-Resolved Fluorescence Anisotropy Decays: Modeling with Classical Simulations

Alvaro J. Lopez,[‡] Emília P. Barros,[†,‡] and Leandro Martínez*

Institute of Chemistry and Center for Computing in Engineering & Science, University of Campinas, 13083-861 Campinas-SP, Brazil

Supporting Information

ABSTRACT: In this work, we discuss the challenging time-resolved fluorescence anisotropy of subtilisin Carlsberg (SC), which contains a single Trp residue and is a model fluorescence system. Experimental decay rates and quenching data suggest that the fluorophore should be exposed to water, but the Trp is partially buried in a hydrophobic pocket in the crystallographic structure. In order to study this inconsistency, molecular dynamics simulations were performed to predict the anisotropy decay rates and emission wavelengths of the Trp. We confirmed the inconsistency of the crystallographic structure with the experimentally observed fluorescence data and performed free energy calculations to show that the buried Trp conformation is 2 orders of magnitude (∼3 kcal/mol) more stable than the solvent-exposed one. However, molecular dynamics simulations in which the Trp side chain was restricted to solvent-exposed conformations displayed a maximum Trp emission wavelength shifted toward lower energies and decay rates compatible with the experimentally probed rates. Therefore, if the solvent-exposed conformations are the most important emitters, the experimental anisotropy can be compatibilized with the crystallographic structure. The most likely explanation is that the fluorescence of the most probable conformation in solution, observed in the crystal, is quenched, and this is consistent with the low quantum yield of Trp113 of SC. Additionally, some experiments might have probed denatured or lysed SC structures. SC anisotropy provides an interesting target for the study of fluorescence anisotropy using simulations, which can be used to test and exemplify how modeling can aid the interpretation of experimental data in a system where structure and solution experiments appear to be inconsistent.

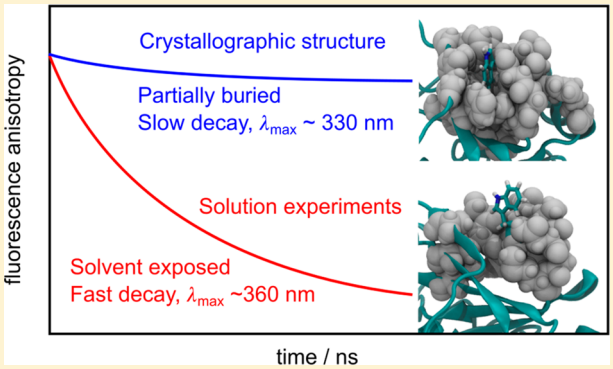

INTRODUCTION

Fluorescence anisotropy decay rates can be used to probe the reorientational dynamics of fluorophores in proteins.[1−3] In principle, they can be computed from classical molecular dynamics simulations (MD).[4−8] In the fluorescence anisotropy phenomenon, an isotropic distribution of fluorescent molecules in solution is excited by plane-polarized light. Those fluorophores with the absorption dipole moments oriented favorably to the polarization and having compatible absorption wavelengths relative to the radiation have the highest probability of transitioning to the excited state. After this photoselection, the excited molecules return to the ground state through the emission of a polarized photon according to the orientation of its emission dipole moment. The degree of polarization of the emission is related to the reorientation of the fluorophores in solution in the time lapse between absorption and emission. This degree of polarization decreases with time as the population of excited fluorophores reorient in solution, and if the system is isotropic, it eventually becomes completely depolarized. The reorientation rate of the fluorophore is dependent on its molecular environment and on the structure to which it might be attached. Thus, this technique is used to probe information on protein local structure and dynamics. Moreover, the solvent affects the reorientational motions, both directly if the fluorophore is exposed to the solution and indirectly through its effect on the viscosity of the solution.[2,4] Therefore, time-resolved fluorescence anisotropy measurements can be used to study the solvation of a protein at a microscopic level.[1,4,8]

The most important fluorophores in proteins are the side chains of tryptophan (Trp) residues. However, since the molecular environment of the Trp side chain affects not only its reorientational dynamics but also its emission wavelength,[9] understanding the experimental results from a molecular perspective is many times complex and dependent on the auxiliary use of modeling methods.[4,8,10] To that end,

Special Issue: Molecular Simulation in Latin America: Coming of Age

Received: July 3, 2019
Published: September 16, 2019

DOI: 10.1021/acs.jcim.9b00539
J. Chem. Inf. Model. 2020, 60, 747−755

simulation strategies to obtain the reorientational dynamics of fluorophores in proteins have been developed.[4,8] The group of Callis, in particular, pioneered the development of hybrid quantum mechanics/molecular mechanics (QM/MM) methodologies for the prediction of fluorescence emission wavelengths and quantum yields.[9−11] Recently, our group developed empirical models to compute fluorescence emission wavelengths of Trp in proteins using classical MD simulations with the aim of providing a practical tool for the interpretation of experimental fluorescence data.[12]

Here we illustrate the importance of modeling methods for the interpretation of fluorophore reorientational dynamics in proteins by a comparative analysis of experimental and computed anisotropy decay rates of the serine protease subtilisin Carlsberg (SC) protein. SC is an important enzyme for industrial applications, and its dynamics in solution has been studied with several methods, such as NMR techniques[13−15] and fluorescence spectroscopy.[16] SC possesses a single Trp residue (Trp113) and has been used as a model system for fluorescence assays.[17−20] The motions of Trp113 are not necessarily associated with the catalytic function of SC,[21] but Trp113 displays complex and interesting fluorescence, and experimental results were variable and subject to continuous debate.[20,22] The crystallographic structure of SC revealed that the Trp113 residue is partially buried in a hydrophobic pocket, as shown in Figure 1A.[23] The maximum

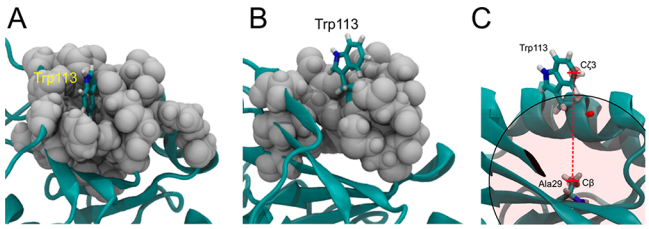

Figure 1. (A) Partially buried tryptophan conformation, as observed in the crystallographic structure and (B) the exposed conformation used to initialize the simulations. (C) Distance used to characterize the exposure of the Trp side chain to the solvent: Ala29-Cβ to Trp113-Cζ3.

fluorescence emission wavelength (λ_{max}) of Trp113 has been shown to be very variable: it is possible to find reported maximum-intensity emissions at 322 nm,[24] 331 nm,[25] 351 nm,[18] 355 nm,[26] and even 360 nm.[22] This variability can be the result of preferential conformations of SC probed by the experiments: greater values of λ_{max} should correspond to solvent-exposed conformations, while shorter wavelengths are characteristic of partially buried conformations.[10−12] The emission wavelength of the crystallographic Trp113 of SC was predicted by Vivian and Callis using QM/MM models[10] and by Lopez and Martínez with classical parametric models.[12] The expected maximum-emission wavelengths were 334 and 337 nm, respectively, consistent with the fact that the Trp113 is partially protected from the solvent.

The great variability of the observed maximum-emission wavelength could also originate from autolysis of the enzyme, releasing into the solution fragments of the protein in which the Trp has a greater quantum yield and emission wavelength.[27] Willis and Szabo also discussed the possibility of interference of Tyr residues in the measured fluorescence spectra, as the quantum yield of Trp113 is low[28] and there are 13 Tyr residues in SC: with excitation at 295 nm and maximum emission at 311 nm, Tyr residues contribute importantly to the fluorescence, but if the excitation is done at 300 nm, only the Trp113 residue is excited, and emission occurs at 322 nm.[27] Therefore, experiments must be performed with great care to guarantee that Trp113 is the major emitting residue.

Experiments to probe the reorientational dynamics of Trp113 by measuring its time-resolved fluorescence anisotropy have been performed by different groups. Lakshmikanth and Krishnamoorthy excited the protein at 295 nm and reported a relatively fast complete depolarization of the fluorescence on the subnanosecond time scale.[26] Janot et al.[20] obtained a lower decay rate on long time scales, consistent with the tumbling motions of a protein of the size of SC. They additionally suggested that much of the fluorescence is quenched and that multiple conformations of Trp113 should be present. Shaw and Pal used 299 nm excitation and reported decay rates similar to those of Janot et al.[18,22] In those experiments, the fluorescence was probed at ∼355 nm, a wavelength that differs significantly from the expected maximum-emission wavelength of the crystallographic Trp113. Quenching assays indicated, in accordance with this choice of λ_{max}, that the probed Trp113 was exposed to water, thus raising further doubts about the consistency of the observations with the crystallographic Trp113 conformation. However, the interpretation of these results is even further complicated by the fact that with excitation at 295 nm the Tyr residues might be important emitters, while this is less likely at 299 nm.

In this work, we provide a molecular description of the role of fluorophore conformational sampling for the reorientational dynamics of SC Trp113. First, we obtain the fluorescence anisotropy decay rates of Trp113 assuming the crystallographic conformation. We observe an inconsistency between experimental and MD-derived anisotropy decays of SC. The time-resolved decays expected from the crystallographic model are much slower than those observed experimentally because the Trp side chain is packed into a hydrophobic pocket, leading to reorientational dynamics on a time scale similar to that of protein tumbling. Using free energy calculations, we confirm that the buried conformation is more favorable in the crystallographic structure but that an open conformation is stable enough to be detected experimentally, for which the emission wavelength of Trp113 is consistent with that probed in the fluorescence anisotropy experiments of Shaw and Pal.[22] MD simulations performed with Trp113 restrained to such conformation show that sampling the appropriate molecular environment results in improved agreement with experimentally observed anisotropy decay rates. We also report the predicted anisotropy decay rates of the SC Tyr residues, which display great variability and could interfere with interpretation of the experiments. We discuss the implications of these results for the interpretation of experimental fluorescence anisotropy experiments for SC and other proteins in general by the use of MD simulations.

MATERIALS AND METHODS

Molecular Dynamics Simulations. MD simulations were performed using standard protocols as follows: The crystallographic structure of SC (PDB ID 1SBC) was used.[23] The protein was solvated in a cubic box of 1.0 g/mL of water with sodium and chloride ions to render the system neutral using PACKMOL.[29,30] The box sides had a length of ∼75 Å, which guaranteed that the Trp113 residue was at least 40 Å apart

DOI: 10.1021/acs.jcim.9b00539
J. Chem. Inf. Model. 2020, 60, 747−755

from periodic images of the protein atoms, safely avoiding boundary effects on its dynamics. The TIP3P model was used for water,[31] and the CHARMM36 force field was used to simulate the protein and ions.[32] Simulations were performed with the NAMD software[33] using a 2 fs time step. Simulations were run at 298.15 K and 1 atm with a 12 Å van der Waals interaction cutoff and the particle mesh Ewald sum[34] for evaluation of the long-range electrostatic potential. Constant temperature and pressure were maintained using a Langevin thermostat[35] (different damping coefficients were used, as discussed in Supporting Information S2, and the figures in the main text report the results obtained with a damping coefficient of 10/ps) and a Langevin barostat[36] with a piston period of 200 fs and a damping time scale of 100 fs. The systems' energies were minimized with 1000 steps of the conjugate-gradient method (CG) and equilibrated with 200 ps of constant-temperature and -pressure MD with the protein fixed, followed by 500 CG steps and 200 ps of MD with the Cα atoms fixed and finally 2 ns of unrestrained MD. Production simulations were then run for 20 ns. Simulations were visualized using VMD.[37] The complete equilibration/production protocol was repeated independently 30 times, and the reported Trp emission wavelengths and decay rates are averages of these 30 realizations.

The crystallographic model of SC displays the side chain of the single tryptophan residue Trp113 inserted in a cavity at the surface of the protein.[23] Time-resolved fluorescence anisotropy curves calculated from simulations generated from this starting structure were greatly distinct from the experimental observations, as will be discussed. Therefore, we generated starting structures with the Trp113 side chain exposed to solvent. For this purpose, a 10 ns simulation with the protein fixed except for the tryptophan side chain was performed in vacuum at 815 K. Frames in which Trp113 was solvent-exposed were selected as starting structures for 10 unrestrained MD simulations using the protocol described above. Besides these unrestrained simulations, we performed additional restrained simulations from the solvent-exposed conformation to prevent the reinsertion of the Trp113 side chain into the hydrophobic pocket: the distance between atoms Cβ of Ala29 and Cζ3 of Trp113 was restricted to a minimum of 12 Å (Figure 1C). This restraint was introduced using the Adaptive Biasing Force (ABF) script, as implemented in NAMD, as follows:[38−40] The reaction coordinate was defined to be the distance above, within minimum and maximum values of 12 and 100 Å. The ABF script introduces a constant restraint potential (a semiharmonic potential with a force constant of 50 kcal mol^{-1} Å^{-2}) that prevents the system from sampling conformations beyond those limits. In an ABF calculation, a force is introduced into the simulation to facilitate the sampling of the reaction coordinate. This was not our intention in this case, and hence, no ABF force was introduced (technically, the force sampling time was set to be larger than the total simulation time), ensuring that the motions of the Trp residue within the limiting values specified were determined by the physical interactions of the molecular system only.

Free Energy Calculations of Trp113 Conformational Equilibrium. In order to determine the relative stabilities of the conformations of the side chain of Trp113, ABF calculations were performed with NAMD.[38−40] As for the restrained simulations, the reaction coordinate was defined as the distance between the Ala29-Cβ and Trp113-Cζ3 atoms. However, the sampled distances ranged from 1.0 to 15.0 Å, in intervals of 0.1 Å. The force constant of the restraining potential was 50 kcal mol^{-1} Å^{-2}. The sampling before the initial application of the ABF force was 500 simulation steps at each reaction coordinate bin. The ABF calculation was repeated independently 20 times. We report the mean profile and the standard error of the mean of these 20 realizations.

Calculation of Fluorescence Anisotropy Decays and Fluorescence Spectra. The time-resolved fluorescence anisotropy $r(t)$ can be computed from the reorientational dynamics of the fluorescent probe.[4,8] It is the ensemble average of the second-order Legendre polynomial $[P_2(x) = {}^1/_2(3x^2 - 1)]$ of the correlation of the angle between the absorption ($\boldsymbol{\mu}_a$) and emission ($\boldsymbol{\mu}_e$) dipole moment vectors. Specifically,

$$r(t) = \frac{2}{5}\langle P_2[\boldsymbol{\mu}_a(s)\cdot\boldsymbol{\mu}_e(s+t)]\rangle \quad (1)$$

where $\langle\cdots\rangle$ indicates an ensemble average for constant t, where t is the time delay relative to the reference instant s. Equation 1 allows the reproduction of the experimental results through MD simulations.[4,8,41] The TCF module of our in-house analysis programs was used for the calculations (http://leandro.iqm.unicamp.br/mdanalysis). The ^1L_a transition dipole moment of Trp was taken as the absorption vector, as it is the preferred transition in polar solutions.[2] It was defined as the vector connecting the center of the bond between carbons Cδ2 and Cε2 of the Trp side chain and the nitrogen in the indole ring. The emission dipole moment was defined as a function of the angle θ with the absorption dipole, calculated from the experimental anisotropy at $t = 0$ (r_0) using[2,42]

$$r_0 = \frac{3\cos^2\theta - 1}{2} \quad (2)$$

Experimental values of r_0 are available for free tryptophan and SC in water.[26]

Nonlinear curve fitting of the anisotropy curves obtained from the simulations was performed to determine the decay rates and weights. The exponential fits were performed on the average decay curves of the 30 independent simulations. Table 1 reports the results of a biexponential curve fitting that assumes two reorientational decay rates, and Table S1 reports a triexponential fit that assumes three independent reorienta-

Table 1. Experimental and Calculated Parameters of the Time-Resolved Fluorescence Anisotropy of Trp113 of subtilisin Carlsberg[a]

	λ_{max} (nm)[b]	r_0	β_1	τ_1 (ns)	β_2	τ_2 (ns)
experimental[26]	355	0.21	0.90	0.17	0.10	3.50
experimental[22]	360	0.22	0.70	0.47	0.30	10−100
crystallographic Trp conformation	333[c] 331[d]	0.19	0.03	1.29	0.97	86
solvent-exposed Trp conformation	355[c] 346[d]	0.18	0.43	0.18	0.57	3−15

[a]Biexponential fits for anisotropy decays were obtained using $r(t) = r_0[\beta_1\exp(-t/\tau_1) + \beta_2\exp(-t/\tau_2)]$, where β_1 and β_2 are scaling factors and τ_1 and τ_2 are the fast and slow characteristic reorientational times, respectively. [b]λ_{max} is the wavelength of maximum fluorescence emission. [c]λ_{max} was computed using a parametric model based on SASA. [d]λ_{max} was computed using a parametric model based on electrostatic interactions.

DOI: 10.1021/acs.jcim.9b00539
J. Chem. Inf. Model. 2020, 60, 747−755

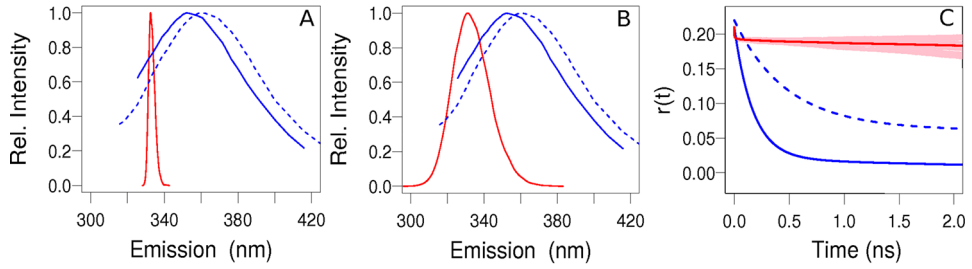

Figure 2. Fluorescence emission wavelengths and anisotropy of the crystallographic conformation of Trp113 of subtilisin Carlsberg. (A, B) Calculated estimates of λ_{max} (red) and experimental fluorescence emission spectra (blue).[22] The λ_{max} estimates were based on (A) the SASA of the indole and (B) electrostatic interactions between indole and water/protein. (C) Calculated (red) and experimental (blue) time-resolved fluorescence anisotropy. Blue continuous and dashed lines correspond to the experimental data from Lakshmikanth and Krishnamoorthy[26] and Shaw and Pal,[22] respectively. Pink lines in (C) show the results of each of the 30 independent simulations.

tional decay rates. The nonlinear fits were obtained using the package minpack.lm available in R.[43]

Fluorescence maximum-emission wavelengths were calculated using classical parametric models 2 and 4 described by Lopez and Martínez.[12] These models allow the prediction of maximum-emission wavelengths based on the solvent-accessible surface area (SASA) of benzene/pyrrole or on the electrostatic interactions of the indole with water and protein atoms. The SASAs of benzene and pyrrole were computed with VMD.[37] Electrostatic interaction energies were computed using our MDAnalysis suite.[44]

RESULTS AND DISCUSSION

Time-Resolved Fluorescence Anisotropy of the Crystallographic Conformation of Trp113. The SC enzyme is an interesting target for the study of fluorescence emission because it contains a single tryptophan residue, Trp113, located close to the protein surface. The fluorescence spectra of SC's Trp113 reported by Lakshmikanth and Krishnamoorthy[26] and by Shaw and Pal[22] exhibit maximum-emission wavelengths of 355 and 360 nm, respectively (Figure 2). These wavelengths indicate that the Trp113 is exposed to water, at least in the conformation that dominates the emission spectra. At the same time, Willis and Szabo[27] reported a maximum-emission wavelength of 322 nm, indicating a Trp113 buried in a hydrophobic pocket, and suggested that the emission at 350 nm could originate from fragments of SC resulting from autolysis.

In the crystal structure of SC, Trp113 is partially buried in a surface-accessible hydrophobic pocket.[23] The expected maximum-emission wavelength of Trp113 in such a molecular environment was predicted to be 337 nm using QM/MM simulations[10] or 331−332 nm using our classical parametric models.[12] Therefore, the experimental and simulation results indicate that there is a conformational heterogeneity of the Trp113 side chain in solution, which is sensitive to experimental conditions to the point that different groups obtain emission spectra consistent with different Trp solvent accessibilities. As we will show, the solvent accessibility of Trp113 completely determines its reorientational dynamics.

Initially we performed molecular dynamics simulations starting from the crystallographic structure of SC and thus with a partially buried Trp113 (Figure 1A). These simulations were used to compute the Trp113 fluorescence wavelength (λ_{max}) and study its conformational dynamics. Figures 2A,B show the experimental fluorescence spectra of SC obtained by Lakshmikanth and Krishnamoorthy[26] and Shaw and Pal,[22] in comparison with the range of λ_{max} computed with our previously reported models based on SASA or electrostatic interactions.[12] The calculated λ_{max} differ from the experimental ones (Figures 2A,B and Table 1). The simulations predict a maximum-emission wavelength for the crystallographic Trp113 that is about 25 nm shorter than that used to probe the reorientational dynamics in fluorescence anisotropy experiments.

Nevertheless, we computed the expected time-resolved fluorescence anisotropy decays of Trp113 resulting from its reorientational dynamics in the simulations generated from the crystallographic conformation. The anisotropy decays predicted from the simulations were greatly distinct from experimental observations, as shown in Figure 2C. MD simulations tend to predict faster decays because of the accelerated diffusion properties of the water model (see Supporting Information S1).[8] In this case, on the contrary, the predicted decays are much slower than the experimentally observed ones. The simulations show that the Trp113 crystallographic conformation implies a reorientational rate similar to that of the overall protein tumbling.

Fluorescence Anisotropy Decay Rates and Solvent Exposure of Trp113. In order to understand the effect of the molecular environment on the reorientational dynamics of the Trp113 side chain, we generated solvent-exposed conformations of this residue from which MD simulations were initiated (see Materials and Methods), as shown in Figure 1B. Initially, 10 independent simulations of 20 ns were performed, and we observed that the Trp113 side chain returned to the crystallographic conformation in the time span of the simulations in six of the 10 runs. The insertion of the side chain into the crystallographic cavity occurred at different instants in each simulation, such that the fraction of time sampled in the crystallographic or solvent-exposed Trp113 conformations was different in each case.

The expected fluorescence anisotropy decays from these simulations are shown in Figure 3. There is a clear correlation between the instant of insertion of the side chain into the crystallographic pocket and the anisotropy decay rate. For instance, in one of the simulations the crystallographic conformation was restored at 1.5 ns, and the anisotropy decay rate computed from this run is similar to that of the crystallographic model, shown in Figure 2C. In this case, the reorientational dynamics of the fluorophore is slow, on the order of the protein tumbling motion. On the other hand, simulations in which the side chain of Trp113 persisted in being exposed to solvent display much faster reorientational dynamics and expected anisotropy decay rates (red lines in the

DOI: 10.1021/acs.jcim.9b00539
J. Chem. Inf. Model. 2020, 60, 747−755

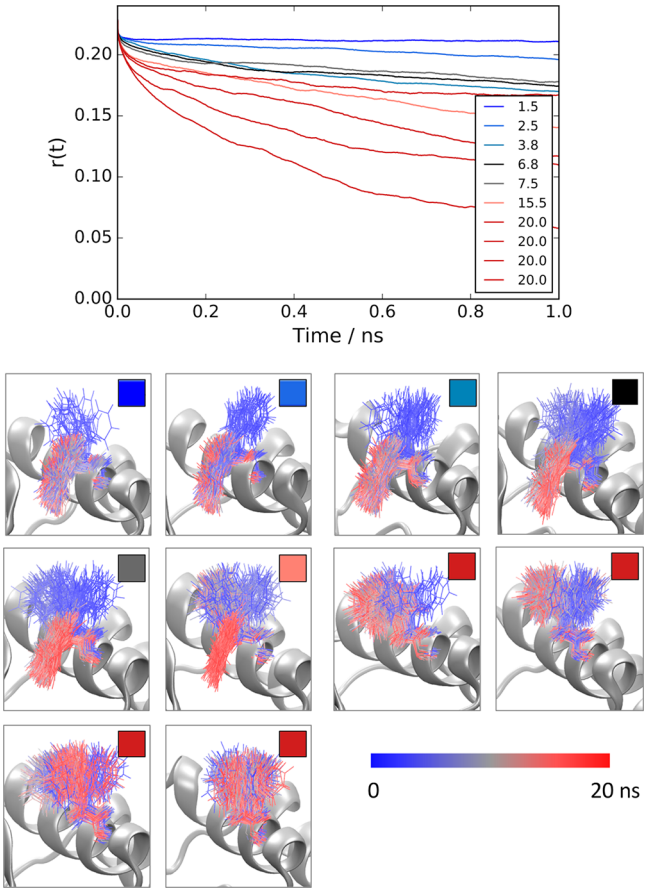

Figure 3. (top) Correlation of the Trp113 side-chain conformation and anisotropy decays from simulations generated from the unrestrained Trp113 solvent-accessible state. From blue to dark red, the colors indicate the instant of insertion of the Trp side chain into the hydrophobic pocket. (bottom) The coordinates of Trp113 at every 0.1 ns of the simulations are shown for each of the 10 runs. The color scale represents the time evolution of the tryptophan position during the course of the simulations.

plot in Figure 3). The greater conformational variability of the side chain of Trp113 in solvent-exposed conformations is evident from visual inspection of the simulations (Figure 3, structural panels). The side chain displays only lateral motions in the crystallographic pocket but is able to rotate in the solvent-exposed conformation.

Relative Stability of the Protected and Solvent-Exposed Trp113 Conformations. The simulations starting with the solvent-exposed conformation of the Trp113 side chain, described in the previous section, indicated that the buried Trp side chain is thermodynamically favored in the crystallographic SC. Therefore, we performed ABF free energy calculations to obtain the relative stabilities of the different Trp113 side-chain solvent exposures. A reaction coordinate (ξ) was defined (see Materials and Methods) such that the solvent-protected side chain is characterized by $\xi \sim 5$ Å and the solvent-exposed side chain is characterized by ξ greater than ~11 Å.

Figure 4 shows the free energy profile of the Trp113 conformations. Two minima were obtained, indicating that the exposure of the Trp113 side chain to water follows a simple conformational equilibrium. The solvent-protected conformation, which is similar to the crystallographic conformation, is preferred. The minimum free energy of the solvent-exposed

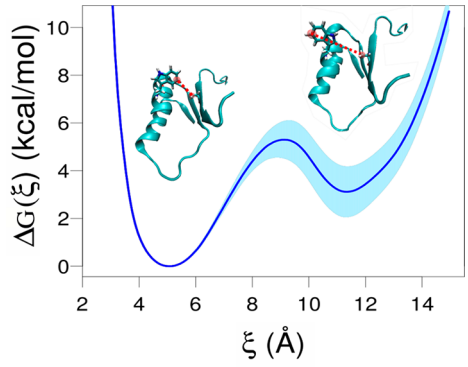

Figure 4. Free energy profile of the conformations adopted by the Trp113 side chain of SC. The reaction coordinate (ξ) is defined as the distance between the Ala29-Cβ and Trp113-Cζ3 atoms. The profile displays two well-defined Trp113 minima, consistent with the solvent-protected side chain (characterized by $\xi \sim 5$ Å) and a solvent-exposed one (at $\xi \sim 11.3$ Å). Twenty independent ABF calculations were performed, and the mean and standard error of the mean (limits of the light-blue region) of the free energy difference relative to the minimum are shown.

conformations is ~3.1 kcal/mol higher than that of the solvent-protected side chain. Therefore, the population of the crystallographic conformation is ~150 times greater than that of the exposed conformation at room temperature.

The energy barrier associated with the transition from the solvent-protected conformation to the solvent-exposed conformation is ~5.3 kcal/mol. On the other hand, the energy barrier for the reverse reaction is much lower (~2.3 kcal/mol). This explains why MD simulations starting with the crystallographic conformation uniquely sample the Trp113 solvent-protected structures. Also, MD runs starting with the solvent-exposed conformation eventually go irreversibly (on the time scale of our simulations) to the crystallographic conformation. The equilibrium dynamics of these conformations impairs the sampling of solvent-exposed structures in conventional simulations.

At the same time, the ~150-fold difference in the populations of the two conformers does not rule out the possibility of the solvent-exposed conformation being dominant for the observed anisotropy if the solvent-protected conformation is significantly quenched. Indeed, this is a possibility discussed by Willis and Szabo[27], and as we will show below, the reorientational motions of solvent-exposed conformations can explain the experimental decays.

Time-Resolved Fluorescence Anisotropy of Solvent-Exposed Trp113. In order to obtain a comprehensive sampling of Trp113 conformations associated with the solvent-exposed scenario, simulations were performed in which the side chain of the fluorophore was restrained to not enter into the crystallographic pocket. The solvent-exposed conformations of Trp113 were used as initial points for the simulations, and the distance between atom Cζ3 of Trp113 and atom Cβ of Ala29 (in the interior of the pocket) was restrained to be greater than 12 Å (Figure 1C). Therefore, these simulations sampled exclusively solvent-exposed Trp113 conformations.

First, the maximum-emission wavelengths of solvent-exposed Trp113 were estimated using parametric models based on SASA or electrostatic interactions of the indole group.[12] The range of estimates of λ_{max} obtained using these

DOI: 10.1021/acs.jcim.9b00539
J. Chem. Inf. Model. 2020, 60, 747−755

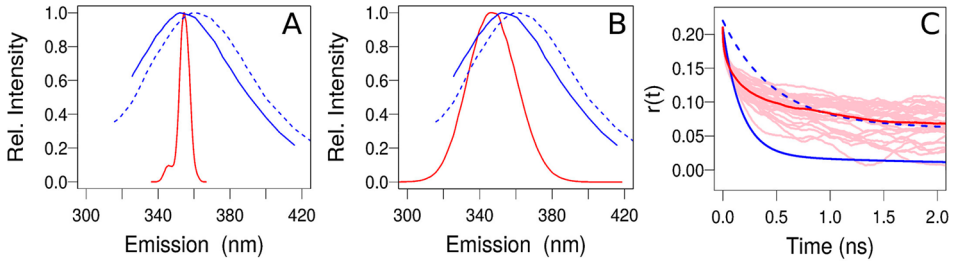

Figure 5. Fluorescence emission wavelengths and anisotropy of the restrained solvent-exposed conformation of Trp113 of subtilisin Carlsberg. (A, B) Calculated estimates of λ_{max} (red) and experimental fluorescence spectra (blue).[22,26] The calculated λ_{max} values were estimated from (A) the SASA of the indole group and (B) electrostatic interactions of the fluorophore side chain with the molecular environment. (C) Calculated (red) and experimental (blue) time-resolved fluorescence anisotropy of the solvent-exposed conformation of Trp113 of subtilisin Carlsberg in water. Blue solid and dashed lines correspond to the experimental data from Lakshmikanth and Krishnamoorthy[26] and Shaw and Pal,[22] respectively.

models are shown in Figure 5A,B, respectively. The most likely maximum-emission wavelengths were 355 and 346 nm (Table 1), which are close to the experimental λ_{max} used to probe the fluorescence anisotropy. The estimated λ_{max} values (346−355 nm) are significantly longer than that expected for Trp113 bound to the crystallographic pocket (331−332 nm). This red shift is expected to result from exposure of the Trp113 side chain to water.

The time-resolved fluorescence anisotropy of SC was then computed from the simulations with Trp113 exposed to water. As shown in Figure 5C, the decays were fast compared with those found for the partially buried conformation of Trp113 of SC (Figure 2C). Table 1 displays the parameters of the biexponential fits of the average anisotropy decay curves from the experimental reference data[22,26] and from the simulations.

The simulated reorientation dynamics has a fast component with a characteristic time of 0.18 ns, which is similar to the fastest component of the fit reported by Lakshmikanth and Krishnamoorthy[26] (0.17 ns). Shaw and Pal,[22] on the other side, reported that the faster decay has a characteristic time of 0.47 ns. Despite the remarkable agreement between the simulations and the results of Lakshmikanth and Krishnamoorthy, the decay rates obtained from simulations are expected to be higher than the experimental ones.[45] Therefore, it is not possible to unambiguously associate this fast component to either of the experimental results.

The slower component of the decay obtained by simulations had a characteristic time ranging between 4 and 20 ns. The fits are not very sensitive to this component, and the experimentally reported values range from 3.50 to 10−100 ns, indistinctly. Most determinant of the overall shape of the anisotropy decay curves are the contributions of the fast and slow components of the complete decays. In the experiments of Lakshmikanth and Krishnamoorthy, the fast component contributes 90% of the decay.[26] This reflects the complete depolarization of the emission that was observed within 2 ns. On the other side, in the work of Shaw and Pal, the fast component is slower and contributes only 47% of the decay, in such a way that within 2 ns there is still a significant polarization of the emitted light.[22]

The simulated decays show that the slow component is mostly associated with the Trp113 conformations in which there are important interactions with the protein. For instance, as shown in Table 1, the fast component of the anisotropy obtained from the crystallographic conformation contributes only 3% of the decay. When the solvent-exposed Trp113 conformation is simulated, this contribution increases to 43%, something similar to the experimental result of Shaw and Pal. Thus, the overall shape of the anisotropy curves is significantly dependent on the conformation of the fluorophore probed. The time dependence of the polarization of the emission is dependent on the extent to which the solvent-exposed conformation of Trp113 is probed relative to the partially buried conformation.

In view of the relative stabilities of the side-chain conformers, as discussed above, significant quenching of the solvent-protected conformation could explain the majority contribution of the more mobile conformers and the difference between the experimental decays and the crystallographic model. Importantly, the quantum yield of Trp113 in the crystallographic SC was estimated to be 0.009,[28] which in the lower limit is about 30 times lower than that of the most efficient Trp emitters in proteins (∼0.31).

The Wobbling-in-a-Cone Model and the Interpretation of Janot et al. The reorientational dynamics of a fluorescent probe with partially restricted motions can be modeled by the wobbling-in-a-cone model.[20,42,46] This model establishes that the fluorophore can diffuse freely inside a cone with semiangle θ_{max} while attached to a larger molecular group with slower reorientational motions. In this case, the anisotropy can be expressed as[20]

$$r(t) = [r_{Trp} \exp(-t/\phi_{Trp}) + r_p] \exp(-t/\phi_p) \quad (3)$$

where ϕ_{Trp} is the correlation time for the motion of the Trp (the fluorophore) in the protein and ϕ_p is the correlation time of the global motion of the protein. The residual anisotropy remaining after faster motions, r_p, can be used to compute the semiangle θ_{max} in which the fluorophore freely wobbles.[20,47]

Janot et al.[20] obtained SC fluorescence anisotropy decays similar to those of Shaw and Pal[22] (see Figure S2) and used the wobbling-in-a-cone model to fit their data. Interestingly, they obtained wobbling angles between 33° and 49°, indicating that the Trp has a relatively wide range of motion.

We fitted the anisotropy decays obtained in our simulations for the crystallographic and solvent-exposed conformations of Trp113 using the same model. For the crystallographic conformation, we obtained θ_{max} = 8.2°, and for the solvent-exposed conformation we obtained θ_{max} = 32°. Thus, the solvent-exposed conformation displays wobbling motions in agreement with those observed by Janot et al., while the motions in the crystallographic conformation are excessively restricted.

Janot et al. noted as well that the high degree of static quenching shown by this Trp residue indicates that it is involved in a complex with a mean lifetime much longer than

DOI: 10.1021/acs.jcim.9b00539
J. Chem. Inf. Model. 2020, 60, 747−755

the nanosecond time scale and suggested that this complex is effectively nonemitting.[20] They concluded that the observed emission appears to result from a small fraction of Trp residues that are free to move in a wide cone semiangle. This interpretation is in complete agreement with the results derived from our simulations. In particular, if the buried conformation is quenched such that its emission is about 2 orders of magnitude less intense than that of the solvent-exposed conformation, the decay would be consistent with the simulated data according to the relative populations we estimated.

Hypotheses for the Conformational Selection of the Solvent-Exposed Trp113. As mentioned in the Introduction, experimental fluorescence spectra of SC have been reported to display maximum-emission wavelengths ranging from 322 to 360 nm.[18,22,24−26] Therefore, SC appears to be able to sample different structures in solution that imply significantly different molecular environments for the Trp113 residue.

In the two reported time-resolved fluorescence anisotropy experiments on Trp113 in SC, a probe emission wavelength was chosen that corresponds to the emission of an indole group significantly exposed to water. Therefore, independent of the particular structure of SC in solution during the fluorescence anisotropy experiments, the emission probed would correspond to the population of solvent-exposed Trp113 residues. Willis and Szabo showed that SC is subject to autolysis and that the emission from fragments of the protein in which Trp113 is released from a quenching environment might be determinant for the observed emission spectra,[27] although the exact mechanism of quenching is not clear from the crystallographic structure.[24] They also showed that with excitation at 295 nm there is still a significant participation of the Tyr residues of SC in the observed fluorescence. We computed the anisotropy decays of all 13 Tyr residues of the protein, and while some are exposed to solvent and reorient at a rate consistent with the results of Shaw and Pal and Janot et al., faster decays consistent with the reorientation rates obtained by Lakshmikanth and Krishnamoorthy are not observed (Supporting Information S3). Since Shaw and Pal excited the protein at 299 nm, the agreement of some of the Tyr decay rates with their result is coincidental only. Therefore, the fluorescence of Tyr residues cannot explain the observed experimental decays.

The experimentally observed decay rates might result from complete or partial denaturation of SC, from autolysis, or from simple exposure of the Trp113 side chain. In fact, Lakshmikanth and Krishnamoorthy prepared the SC solution also under denaturing conditions and did not observe a significant change in the emission wavelength of Trp113.[26] The minor contribution of the tumbling decay rate to their result might be indicative of the presence of a significant population of denatured or lysed SC molecules. On the other hand, the anisotropy decay rates obtained by Shaw and Pal[22] and Janot et al.[20] display an important tumbling component that prevents the anisotropy from decaying completely on the time scale of the experiments. Additionally, the enzyme was shown to be active under the experimental conditions probed, such that at least a significant population of native structures was present. Nevertheless, they reported Trp113 to emit at a wavelength also consistent with solvent exposure.

Therefore, the inconsistency between the experimental anisotropy decays and those predicted from the crystallographic conformation might have different origins: (1) the Trp113 emission is quenched in the crystallographic pocket, such that the most important observed emission results from the minor solvent-exposed conformations resulting from local side-chain motions, and (2) partial denaturation or autolysis can produce populations of solvent-exposed side chains that dominate the fluorescence. Indeed, Willis and Szabo[27] showed that without purification the fluorescence displays a marked red shift but also an increased emission intensity, supporting the contamination hypothesis.

Our simulations indicate that the first hypothesis is sufficient to explain quite reasonably the experimental anisotropy decays of Shaw and Pal and Janot et al. by probing only the fluorescence of locally exposed side chains in a mostly preserved protein structure. This hypothesis is consistent with the verified activity of SC in these experiments and supported by the low quantum yield of the Trp113 side chain. The second hypothesis is probably necessary to explain why the emission is completely depolarized in less than 2 ns in the experiments of Lakshmikanth and Krishnamoorthy.

CONCLUSIONS

The present work aimed at the reproduction of the time-resolved fluorescence anisotropy decay of Trp113 of subtilisin Carlsberg. The simulations show that the stable crystallographic conformation of the Trp side chain implies fluorescence anisotropy decays much slower than the experimentally observed ones. In the pocket-bound conformation, the reorientation dynamics of the Trp side chain follows that of the protein, and the expected anisotropy decay would be similar to the one implied by protein tumbling. Experimentally, however, much higher decay rates were observed, and quenching experiments suggested that the fluorescent Trp side chain was exposed to solvent. Therefore, there is an inconsistency between the experimentally probed structure in solution and the crystallographic-like structure of SC. We have shown that the population of solvent-exposed conformations is about 2 orders of magnitude smaller than that of the solvent-protected side chain but still relevant. To overcome the inconsistency of the experimental decays and the crystallographic model, solvent-exposed Trp conformations, which are predicted to emit at the experimentally probed wavelengths, were sampled by molecular dynamics simulations. In this case, we obtained faster decays, improving the consistency with the experimental data. Therefore, quenching of the solvent-protected conformation or some local structural fluctuation favoring the exposure of the side chain is sufficient to reconcile the crystallographic model and the observed anisotropy. To effectively compare experiments and simulations, here we have explored a combination of methodologies that from classical protein simulations provide emission wavelengths and anisotropies. These methods can predict the time-resolved fluorescence anisotropy of Trp in proteins and provide a molecular basis for experimental observations.

ASSOCIATED CONTENT

Supporting Information

The Supporting Information is available free of charge on the ACS Publications website at DOI: 10.1021/acs.jcim.9b00539.

Comparison between calculated and experimental anisotropy decay and fluorescence emission wavelength of free tryptophan in water, analysis of the dependence

DOI: 10.1021/acs.jcim.9b00539
J. Chem. Inf. Model. 2020, 60, 747−755

of the anisotropy decay rates at different Langevin damping coefficients (0.01, 1.0, and 10 ps^{-1}), effect of the simulation time on the calculated anisotropy rates, and analysis of the anisotropy decay rates of each tyrosine residue (PDF)

AUTHOR INFORMATION

Corresponding Author

*E-mail: leandro@iqm.unicamp.br.

ORCID

Alvaro J. Lopez: 0000-0002-6073-6058

Leandro Martínez: 0000-0002-6857-1884

Present Address

†E.P.B.: Department of Chemistry and Biochemistry, University of California, San Diego, 9500 Gilman Drive, La Jolla, California 92093-0378, United States.

Author Contributions

‡A.J.L. and E.P.B. contributed equally.

Notes

The authors declare no competing financial interest.

ACKNOWLEDGMENTS

The authors thank the funding agencies Fapesp (Grants 2010/16947-9, 2018/24293-0, and 2013/08293-7) and CNPq (Grants 302332/2016-2 and 161789/2014-5) for financial support.

REFERENCES

(1) Bucci, E.; Steiner, R. F. Anisotropy Decay of Fluorescence as an Experimental Approach to Protein Dynamics. *Biophys. Chem.* **1988**, *30*, 199−224.

(2) Lakowicz, J. R. *Principles of Fluorescence Spectroscopy*; Springer Science & Business Media, 2007.

(3) Cross, A. J.; Fleming, G. R. Analysis of Time-Resolved Fluorescence Anisotropy Decays. *Biophys. J.* **1984**, *46*, 45−56.

(4) Schröder, G. F.; Alexiev, U.; Grubmüller, H. Simulation of Fluorescence Anisotropy Experiments: Probing Protein Dynamics. *Biophys. J.* **2005**, *89*, 3757−3770.

(5) Suzuki, S.; Sakai, F.; Hasegawa, S.; Miyata, T.; Harakuni, T.; Yamaguchi, R.; Arakawa, T. Fluorescence Anisotropy Measurement of Green Fluorescent Protein for Nano-Environment Probing. In *2013 6th Biomedical Engineering International Conference (BMEiCON 2013)*; IEEE, 2013; pp 105−108.

(6) Košovan, P.; Limpouchová, Z.; Procházka, K. Molecular Dynamics Simulation of Time-Resolved Fluorescence Anisotropy Decays from Labeled Polyelectrolyte Chains. *Macromolecules* **2006**, *39*, 3458−3465.

(7) Axelsen, P. H.; Haydock, C.; Prendergast, F. G. Molecular Dynamics of Tryptophan in Ribonuclease-T1. I. Simulation Strategies and Fluorescence Anisotropy Decay. *Biophys. J.* **1988**, *54*, 249−258.

(8) Batista, M. R. B.; Martínez, L. Dynamics of Nuclear Receptor Helix-12 Switch of Transcription Activation by Modeling Time-Resolved Fluorescence Anisotropy Decays. *Biophys. J.* **2013**, *105*, 1670−1680.

(9) Callis, P. R. Exploring the Electrostatic Landscape of Proteins with Tryptophan Fluorescence. *Rev. Fluoresc.* **2009**, *2007*, 199−248.

(10) Vivian, J. T.; Callis, P. R. Mechanisms of Tryptophan Fluorescence Shifts in Proteins. *Biophys. J.* **2001**, *80*, 2093−2109.

(11) Callis, P. R.; Burgess, B. K. Tryptophan Fluorescence Shifts in Proteins from Hybrid Simulations: An Electrostatic Approach. *J. Phys. Chem. B* **1997**, *101*, 9429−9432.

(12) Lopez, A. J.; Martínez, L. Parametric Models to Compute Tryptophan Fluorescence Wavelengths from Classical Protein Simulations. *J. Comput. Chem.* **2018**, *39*, 1249−1258.

(13) Hutcheon, G. A.; Parker, M. C.; Moore, B. D. Measuring Enzyme Motility in Organic Media Using Novel H-D Exchange Methodology. *Biotechnol. Bioeng.* **2000**, *70*, 262−269.

(14) Hudson, E. P.; Eppler, R. K.; Beaudoin, J. M.; Dordick, J. S.; Reimer, J. A.; Clark, D. S. Active-Site Motions and Polarity Enhance Catalytic Turnover of Hydrated Subtilisin Dissolved in Organic Solvents. *J. Am. Chem. Soc.* **2009**, *131*, 4294−4300.

(15) Partridge, J.; Dennison, P. R.; Moore, B. D.; Halling, P. J. Activity and Mobility of Subtilisin in Low Water Organic Media: Hydration Is More Important than Solvent Dielectric. *Biochim. Biophys. Acta, Protein Struct. Mol. Enzymol.* **1998**, *1386*, 79−89.

(16) Halle, B. Protein Hydration Dynamics in Solution: A Critical Survey. *Philos. Trans. R. Soc., B* **2004**, *359*, 1207−1223.

(17) Castro, G. R. Enzymatic Activities of Proteases Dissolved in Organic Solvents. *Enzyme Microb. Technol.* **1999**, *25*, 689−694.

(18) Pal, S. K.; Peon, J.; Zewail, A. H. Biological Water at the Protein Surface: Dynamical Solvation Probed Directly with Femtosecond Resolution. *Proc. Natl. Acad. Sci. U. S. A.* **2002**, *99*, 1763−1768.

(19) Kamal, J. K. A.; Xia, T.; Pal, S. K.; Zhao, L.; Zewail, A. H. Enzyme Functionality and Solvation of Subtilisin Carlsberg: From Hours to Femtoseconds. *Chem. Phys. Lett.* **2004**, *387*, 209−215.

(20) Janot, J. M.; Beeby, A.; Bayley, P. M.; Phillips, D. The Time Resolved Fluorescence and Anisotropy of Subtilisins BPN′ and Carlsberg. *Biophys. Chem.* **1991**, *41*, 277−287.

(21) Warshel, A.; Bora, R. P. Perspective: Defining and Quantifying the Role of Dynamics in Enzyme Catalysis. *J. Chem. Phys.* **2016**, *144*, 180901.

(22) Shaw, A. K.; Pal, S. K. Activity of Subtilisin Carlsberg in Macromolecular Crowding. *J. Photochem. Photobiol., B* **2007**, *86*, 199−206.

(23) Neidhart, D. J.; Petsko, G. A. The Refined Crystal Structure of Subtilisin Carlsberg at 2.5 Å Resolution. *Protein Eng., Des. Sel.* **1988**, *2*, 271−276.

(24) Eftink, M. R. Fluorescence Techniques for Studying Protein Structure. *Methods Biochem. Anal.* **2006**, *35*, 127−205.

(25) Bayley, P. M.; Janot, J.-M.; Martin, S. R. Subtilisin Enzymes: A Note on Time-Resolved Fluorescence and Circular Dichroism Properties. *FEBS Lett.* **1989**, *250*, 389−394.

(26) Lakshmikanth, G. S.; Krishnamoorthy, G. Solvent-Exposed Tryptophans Probe the Dynamics at Protein Surfaces. *Biophys. J.* **1999**, *77*, 1100−1106.

(27) Willis, K. J.; Szabo, A. G. Resolution of Tyrosyl and Tryptophyl Fluorescence Emission from Subtilisins. *Biochemistry* **1989**, *28*, 4902−4908.

(28) Callis, P. R.; Liu, T. Quantitative Prediction of Fluorescence Quantum Yields for Tryptophan in Proteins. *J. Phys. Chem. B* **2004**, *108*, 4248−4259.

(29) Martínez, L.; Andrade, R.; Birgin, E. G.; Martínez, J. M. PACKMOL: A Package for Building Initial Configurations for Molecular Dynamics Simulations. *J. Comput. Chem.* **2009**, *30*, 2157−2164.

(30) Martínez, J. M.; Martínez, L. Packing Optimization for Automated Generation of Complex System's Initial Configurations for Molecular Dynamics and Docking. *J. Comput. Chem.* **2003**, *24*, 819−825.

(31) Jorgensen, W. L.; Chandrasekhar, J.; Madura, J. D.; Impey, R. W.; Klein, M. L. Comparison of Simple Potential Functions for Simulating Liquid Water. *J. Chem. Phys.* **1983**, *79*, 926−935.

(32) MacKerell, A. D.; Bashford, D.; Bellott, M.; Dunbrack, R. L.; Evanseck, J. D.; Field, M. J.; Fischer, S.; Gao, J.; Guo, H.; Ha, S.; et al. All-Atom Empirical Potential for Molecular Modeling and Dynamics Studies of Proteins. *J. Phys. Chem. B* **1998**, *102*, 3586−3616.

(33) Phillips, J. C.; Braun, R.; Wang, W.; Gumbart, J.; Tajkhorshid, E.; Villa, E.; Chipot, C.; Skeel, R. D.; Kalé, L.; Schulten, K. Scalable Molecular Dynamics with NAMD. *J. Comput. Chem.* **2005**, *26*, 1781−1802.

DOI: 10.1021/acs.jcim.9b00539
J. Chem. Inf. Model. 2020, 60, 747−755

(34) Darden, T.; York, D.; Pedersen, L. Particle Mesh Ewald: An *N*·log(*N*) Method for Ewald Sums in Large Systems. *J. Chem. Phys.* **1993**, *98*, 10089−10092.
(35) Brünger, A.; Brooks, C. L.; Karplus, M. Stochastic Boundary Conditions for Molecular Dynamics Simulations of ST2 Water. *Chem. Phys. Lett.* **1984**, *105*, 495−500.
(36) Martyna, G. J.; Tobias, D. J.; Klein, M. L. Constant Pressure Molecular Dynamics Algorithms. *J. Chem. Phys.* **1994**, *101*, 4177−4189.
(37) Humphrey, W.; Dalke, A.; Schulten, K. VMD: Visual Molecular Dynamics. *J. Mol. Graphics* **1996**, *14*, 33−38.
(38) Pohorille, A.; Jarzynski, C.; Chipot, C. Good Practices in Free-Energy Calculations. *J. Phys. Chem. B* **2010**, *114*, 10235−10253.
(39) Hénin, J.; Fiorin, G.; Chipot, C.; Klein, M. L. Exploring Multidimensional Free Energy Landscapes Using Time-Dependent Biases on Collective Variables. *J. Chem. Theory Comput.* **2010**, *6*, 35−47.
(40) Darve, E.; Rodríguez-Gómez, D.; Pohorille, A. Adaptive Biasing Force Method for Scalar and Vector Free Energy Calculations. *J. Chem. Phys.* **2008**, *128*, 144120.
(41) Scott, D. R.; Vardeman, C. F., 2nd; Corcelli, S. A.; Baker, B. M. Limitations of Time-Resolved Fluorescence Suggested by Molecular Simulations: Assessing the Dynamics of T Cell Receptor Binding Loops. *Biophys. J.* **2012**, *103*, 2532−2540.
(42) Ichiye, T.; Karplus, M. Fluorescence Depolarization of Tryptophan Residues in Proteins: A Molecular Dynamics Study. *Biochemistry* **1983**, *22*, 2884−2893.
(43) Bloomfield, V. A. *Using R for Numerical Analysis in Science and Engineering*; CRC Press, 2018.
(44) Martínez, L. MDAnalysis, version 17.224. http://leandro.iqm.unicamp.br/mdanalysis.
(45) Doshi, U.; Hamelberg, D. Extracting Realistic Kinetics of Rare Activated Processes from Accelerated Molecular Dynamics Using Kramers' Theory. *J. Chem. Theory Comput.* **2011**, *7*, 575−581.
(46) Babcock, J. J.; Brancaleon, L. The Effect of Local Dynamics of Atto 390-Labeled Lysozyme on Fluorescence Anisotropy Modeling. *Biopolymers* **2015**, *103*, 285−295.
(47) Kinosita, K.; Ikegami, A.; Kawato, S. On the Wobbling-in-Cone Analysis of Fluorescence Anisotropy Decay. *Biophys. J.* **1982**, *37*, 461−464.

DOI: 10.1021/acs.jcim.9b00539
J. Chem. Inf. Model. 2020, 60, 747−755